Exact solution of a restricted Euler equation for the velocity gradient tensor

Brian J. Cantwell
Department of Aeronautics and Astronautics, Stanford University, Stanford, California 94305

(Received 30 July 1991; accepted 14 November 1991)

The velocity gradient tensor satisfies a nonlinear evolution equation of the form $(dA_{ij}/dt) + A_{ik}A_{kj} - (1/3)(A_{mn}A_{nm})\delta_{ij} = H_{ij}$, where $A_{ij} = \partial u_i/\partial x_j$ and the tensor H_{ij} contains terms involving the action of cross derivatives of the pressure field and viscous diffusion of the velocity gradient. The homogeneous case ($H_{ij} = 0$) considered previously by Vielliefosse [J. Phys. (Paris) **43**, 837 (1982); Physica A **125**, 150 (1984)] is revisited here and examined in the context of an exact solution. First the equations are simplified to a linear, second-order system $(d^2A_{ij}/dt^2) + (2/3)Q(t)A_{ij} = 0$, where $Q(t)$ is expressed in terms of Jacobian elliptic functions. The exact solution in analytical form is then presented providing a detailed description of the relationship between initial conditions and the evolution of the velocity gradient tensor and associated strain and rotation tensors. The fact that the solution satisfies both a linear second-order system and a nonlinear first-order system places certain restrictions on the solution path and leads to an asymptotic velocity gradient field with a geometry that is largely but not wholly independent of initial conditions and an asymptotic vorticity which is proportional to the asymptotic rate of strain. A number of the geometrical features of fine-scale motions observed in direct numerical simulations of homogeneous and inhomogeneous turbulence are reproduced by the solution of the $H_{ij} = 0$ case.

I. INTRODUCTION

Dimensional arguments applied to the transport equation for turbulent kinetic energy lead to the conclusion that instantaneous velocity gradients in a turbulent flow are larger than mean gradients by at least a factor of order $\sqrt{R_\delta}$ where R_δ is a Reynolds number based on integral length and velocity scales. Since velocity fluctuations are limited by the mean flow, large velocity gradients must occur in microscale regions whose characteristic length is much smaller than the mean flow. Fluctuations in the instantaneous velocity gradient contribute nothing to the mean transport of momentum because of the linearity of the viscous stress term in the Navier–Stokes equations. However, fluctuating gradients contribute a dominant portion of the kinetic energy dissipation which is quadratic in the strain rate. Thus the fine-scale structure of a turbulent flow plays a key role in the balance of turbulent kinetic energy. For this reason there is currently a considerable amount of research directed at gaining a better understanding of the instantaneous velocity gradient field.

It is exceedingly difficult to directly measure instantaneous velocity gradients in the laboratory because of the high spatial resolution required. The recent availability of direct numerical simulations of turbulent flows at moderate Reynolds numbers has provided a new avenue of approach that permits the study of all nine components of the velocity gradient tensor as well as various other quantities which contribute to the source term H_{ij}.

The case $H_{ij} = 0$ was first studied by Vielliefosse[1,2] who showed that solutions become singular in a finite time and that as time reaches its maximum value there is a tendency for the velocity gradient field to approach a state where two of the principal rates of strain are positive and one is negative and the vorticity vector is aligned with the intermediate principal strain direction. In the earlier study these results were deduced by neglecting the nonlinear convective terms in the substantial derivative of the velocity gradient tensor. In the later study this was corrected and the results were interpreted to apply in a frame of reference moving with a fluid particle. The previous results were reproduced using an asymptotic analysis based in nonorthogonal coordinates aligned with the eigenvectors of the velocity gradient tensor. Interest in this problem was heightened when it was found by Ashurst *et al.*[3] that the geometry of fine-scale motions in isotropic turbulence forced at low wave number exhibited a number of trends in common with the results of Vielliefosse. Since then these trends have been observed in several recent studies of isotropic turbulence including the work of Vincent and Menguzzi[4] and Ruetsch and Maxey.[5] While emphasizing the limitations imposed by the assumption $H_{ij} = 0$, Pumir and Siggia[6] note similar trends in a numerical study of the Euler equations designed to search for the onset of singularities. Reference is also made here to the work of Girimaji and Pope[7] who use the results of direct numerical simulation to develop a stochastic model of H_{ij} which is intended to provide a realistic treatment of the behavior of the velocity gradient tensor in isotropic turbulence.

Recently the same trends have been observed in direct simulations of inhomogeneous flows. Chen *et al.*[8] and Sondergaard, *et al.*[9] studied direct numerical simulations of shear flows including incompressible and weakly compressible time developing mixing layers and wakes and found a strong tendency for the velocity gradient field to approach a state where two of the principal rates of strain are positive

 0899-8213/92/040782-12$04.00

and one is negative and the vorticity vector is aligned with the intermediate principal strain direction. In addition the vorticity and strain were found to have comparable magnitude. This tendency was found to be more pronounced as the Reynolds number was increased and the alignment of the vorticity vector with the intermediate positive strain direction was found to be more exact as the sample was conditioned on higher and higher dissipation rates. Thus in spite of the severe limitations imposed by the assumption $H_{ij}=0$, the solutions of the restricted Euler system have some features in common with numerical simulations using the full equations of motion. In this regard the exact solution of the problem is of some interest. The convenience of an exact solution precludes the need to work in nonorthogonal coordinates and leads to a detailed description of the relationship between initial conditions and the evolution of the velocity gradient tensor and associated strain and rotation tensors.

II. PROBLEM FORMULATION

The Navier–Stokes equations

$$\frac{\partial u_i}{\partial t}+u_k\frac{\partial u_i}{\partial x_k}=-\frac{\partial p}{\partial x_i}+\nu\frac{\partial^2 u_i}{\partial x_k\,\partial x_k} \tag{1}$$

are differentiated with respect to x_j leading to

$$\frac{\partial}{\partial t}(A_{ij})+u_k\frac{\partial}{\partial x_k}(A_{ij})+A_{ik}A_{kj} =-\frac{\partial^2 p}{\partial x_i\,\partial x_j}+\nu\frac{\partial^2 A_{ij}}{\partial x_k\partial x_k};\quad i,j=1,2,3, \tag{2}$$

where A_{ij} is the velocity gradient tensor, $A_{ij}=\partial u_i/\partial x_j$. Using the incompressibility condition $A_{ii}=0$, the pressure is given by

$$A_{ik}A_{ki}=-\frac{\partial^2 p}{\partial x_i\,\partial x_i}. \tag{3}$$

Subtracting (3) from (2) with the condition that the trace of the pressure term be zero produces

$$\frac{\partial A_{ij}}{\partial t}+u_k\frac{\partial A_{ij}}{\partial x_k}+A_{ik}A_{kj}-(A_{km}A_{mk})\frac{\delta_{ij}}{3}=H_{ij}, \tag{4}$$

where δ_{ij} is the Kronecker delta and

$$H_{ij}=-\left(\frac{\partial^2 p}{\partial x_i\,\partial x_j}-\frac{\partial^2 p}{\partial x_k\,\partial x_k}\frac{\delta_{ij}}{3}\right)+\nu\frac{\partial^2 A_{ij}}{\partial x_k\,\partial x_k}. \tag{5}$$

Setting $H_{ij}=0$ removes source terms involving spatial derivatives and the natural setting for the homogeneous problem is in terms of a Lagrangian system of coordinates moving with a fluid particle. The local gradient field evolves according to the following ninth-order system of ordinary differential equations:

$$\frac{dA_{ij}}{dt}+A_{ik}A_{kj}-(A_{km}A_{mk})\frac{\delta_{ij}}{3}=0, \tag{6}$$

subject to the incompressibility condition. Equation (6) is a matrix Ricatti equation that can be transformed to a linear second-order system. Linear gradients in the pressure field which might arise due to acceleration of the frame of reference will not appear in (5) and so the reduction to (6) retains the invariance under nonuniform translation of the original system (1). Nevertheless, removal of H_{ij}, particularly the pressure term, is a drastic simplification that effectively takes away the possibility for the motion of adjacent particles to affect one another through the pressure-viscous-stress field. In this model all particles in the field evolve independently.

Evolution equations for the invariants of the velocity gradient tensor are derived by forming appropriate products with (4) and taking the trace. Retaining H_{ij} for the moment, transport equations for the double products and triple products of A_{ij} are

$$\frac{d}{dt}(A_{in}A_{nj})+2A_{in}A_{nk}A_{kj}-\frac{2}{3}(A_{km}A_{mk})A_{ij} =A_{in}H_{nj}+H_{in}A_{nj} \tag{7}$$

and

$$\frac{d}{dt}(A_{iq}A_{qn}A_{nj})+3A_{iq}A_{qn}A_{nk}A_{kj}-(A_{nm}A_{mn})A_{iq}A_{qj} =A_{in}A_{nk}H_{kj}+A_{in}H_{nk}A_{kj}+H_{in}A_{nk}A_{kj}. \tag{8}$$

The eigenvalues of A_{ij} satisfy the characteristic equation

$$\lambda^3+P\lambda^2+Q\lambda+R=0 \tag{9}$$

and, by the Cayley–Hamilton theorem, the matrix A_{ij} satisfies

$$A_{im}A_{mk}A_{kj}+PA_{ik}A_{kj}+QA_{ij}+R\delta_{ij}=0. \tag{10}$$

For the case of incompressible flow, the invariants of the velocity gradient tensor are

$$P=-A_{ii}=0,\quad Q=-\tfrac{1}{2}A_{im}A_{mi},\quad R=-\tfrac{1}{3}A_{im}A_{mk}A_{ki}. \tag{11}$$

Taking the trace of (7) leads to

$$\frac{dQ}{dt}+3R=-A_{ik}H_{ki}. \tag{12}$$

The Cayley–Hamilton relation (10) is used to reduce fourth-order products in (8) to second-order products multiplying Q. Taking the trace of the result leads to

$$\frac{dR}{dt}-\frac{2}{3}Q^2=-A_{in}A_{nm}H_{mi}. \tag{13}$$

The solutions of (12) and (13) for $H_{ij}=0$, which will be presented in the next section, are expressed in terms of Jacobian elliptic functions of the first kind. First we complete the simplification of the system (4).

Differentiating (4) with respect to time leads to

$$\frac{d^2A_{ij}}{dt^2}+A_{ik}\frac{dA_{kj}}{dt}+\frac{dA_{ik}}{dt}A_{kj}+\frac{2}{3}\frac{dQ}{dt}\delta_{ij}=\frac{dH_{ij}}{dt}. \tag{14}$$

Substituting (4) back into (14) gives

$$\frac{d^2A_{ij}}{dt^2}+A_{ik}\left(-A_{kn}A_{nj}-\frac{2}{3}Q\delta_{kj}+H_{kj}\right) +\left(-A_{in}A_{nk}-\frac{2}{3}Q\delta_{ik}+H_{ik}\right)A_{kj} +\frac{2}{3}(-3R-A_{nm}H_{mn})\delta_{ij}=\frac{dH_{ij}}{dt}. \tag{15}$$

Now (10) is used to replace triple products leading to the following second-order system for A_{ij}:

$$\frac{d^2A_{ij}}{dt^2}+\frac{2}{3}Q(t)A_{ij}=\frac{dH_{ij}}{dt}-A_{ik}H_{kj}-H_{ik}A_{kj}+\frac{2}{3}(A_{nm}H_{mn})\delta_{ij}. \tag{16}$$

With the assumption $H_{ij}=0$ for all time, the system (16) completely decouples and all nine components of the velocity gradient tensor satisfy the same linear, second-order Hill equation with function $Q(t)$, singular at the two ends of a finite interval in time. Equations (12) and (13) are solved for Q and R and then the result for Q is used in (16) to solve for the various A_{ij}.

III. SOLUTION OF Q VS R

Elimination of dt between Eqs. (12) and (13) and integration of the result leads to the family

$$\tfrac{27}{4}R^2+Q^3=Q|^3_{R=0} \tag{17}$$

shown in Fig. 1(a). The direction arrows in this figure denote increasing time.

The solution curves (17) have been parametrized in terms of the value of Q when $R=0$ which will hereafter be called Q_0. Note that $Q_0=0$ corresponds to

$$R=\pm(-\tfrac{4}{27}Q^3)^{1/2},\quad Q=-(\tfrac{27}{4}R^2)^{1/3}, \tag{18}$$

which happens to be the boundary across which the eigenvalues of the velocity gradient tensor defined by (9) change from real to complex. It is not obvious that this should be so and another choice of the model equation (6) would generate a different result. For example the factor (1/3) which appears in the fourth term in Eq. (4) is chosen to make the trace of H_{ij} equal to zero and could have been chosen to have a different value in which case the functions $Q(t)$ and $R(t)$ would not conform to the asymptotes (18). For $Q_0>0$ the eigenvalues of (9) are complex. For $Q_0<0$ the eigenvalues are real and for $Q_0=0$ the eigenvalues are real and two are equal. Solving (17) for the third invariant R,

$$R=\pm\frac{2}{3\sqrt{3}}(Q_0^3-Q^3)^{1/2}. \tag{19}$$

Note that the expression in parentheses is always positive.

It is important to distinguish between solutions corresponding to positive, negative, and zero values of Q_0. First, all variables are nondimensionalized. Let

$$q=Qt_0^2,\quad r=Rt_0^3,\quad a_{ij}=A_{ij}t_0,\quad \tau=t/t_0, \tag{20}$$

where t_0 is a characteristic time of the system defined by

$$t_0=1/\sqrt{\mathrm{abs}(Q_0)}. \tag{21}$$

In the special case where $Q_0=0$, the nondimensionalization is carried out using Q_i, the initial value of Q. In this case

$$t_0=1/\sqrt{-Q_i}. \tag{22}$$

In dimensionless form the evolution equations (12), (13), and (16) are

$$\frac{dq}{d\tau}=-3r, \tag{23}$$

$$\frac{dr}{d\tau}=\frac{2}{3}q^2, \tag{24}$$

and

$$\frac{d^2a_{ij}}{d\tau^2}+\frac{2}{3}q(\tau)a_{ij}=0,\quad i,j=1,2,3, \tag{25}$$

and the family (17) becomes

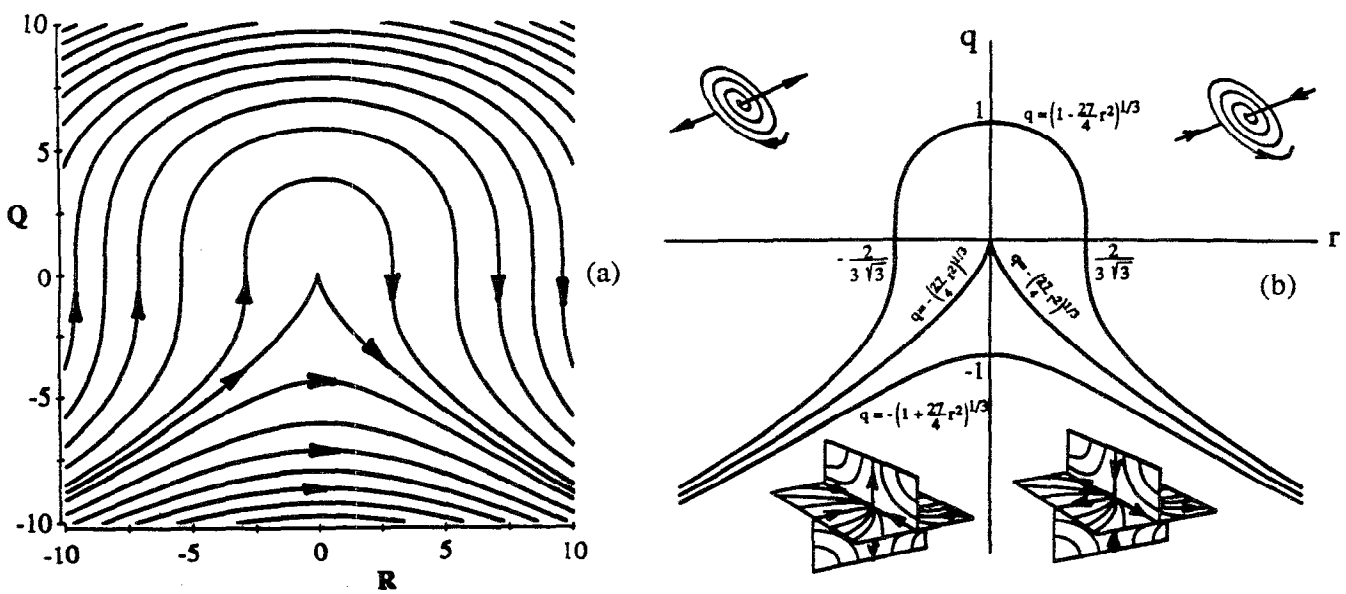

FIG. 1. Trajectories of the invariants of the velocity gradient tensor: (a) dimensioned Q vs R, (b) dimensionless q vs r with schematic diagrams of local streamlines.

$$\tfrac{27}{4}r^2 + q^3 = \mathrm{sgn}(Q_0), \tag{26}$$

where

$$\mathrm{sgn}(Q_0) = \begin{pmatrix} +1; & Q_0 > 0 \\ -1; & Q_0 < 0 \\ 0; & Q_0 = 0 \end{pmatrix}. \tag{27}$$

The three branches of (26) are shown in Fig. 1(b). In addition, Fig. 1(b) schematically depicts solution trajectories corresponding to various possible values of q and r. These are local streamline patterns as they would be seen by a moving observer with the origin of coordinates attached to a fluid particle. The patterns are generated by integrating the linear system of equations in x, y, and z produced by truncating, at the lowest order, a Taylor series expansion of the velocity field about the point in question. The coefficients of this expansion are the components of the velocity gradient tensor evaluated at the point. It is noted that, while given values of q and r imply the local flow patterns depicted in Fig. 1(b), there are no implications in these patterns for the tensor H_{ij} which requires information about the spatial derivatives of A_{ij}.

IV. THE FUNCTIONS $q(\tau)$ AND $r(\tau)$

Using (26), Eq. (23) becomes

$$\begin{aligned} \frac{dq}{d\tau} &= +\frac{2}{\sqrt{3}}\left[\mathrm{sgn}(Q_0) - q^3\right]^{1/2} \quad (r<0), \\ \frac{dq}{d\tau} &= -\frac{2}{\sqrt{3}}\left[\mathrm{sgn}(Q_0) - q^3\right]^{1/2} \quad (r>0), \end{aligned} \tag{28}$$

which is solved in terms of elliptic integrals (Gradshteyn and Ryzhik,[10] item 3.139 p. 229):

$$\begin{aligned} (3)^{1/4}\int_{-\infty}^{q} \frac{dq}{(1-q^3)^{1/2}} &= F\left(\alpha, \sin\frac{5\pi}{12}\right) = \frac{2}{(3)^{1/4}}\tau; \\ & Q_0 > 0; \quad -\infty < q < 1, \\ (3)^{1/4}\int_{q}^{-1} \frac{dq}{(-q^3-1)^{1/2}} &= F\left(\gamma, \sin\frac{\pi}{12}\right) = \frac{2}{(3)^{1/4}}\tau; \\ & Q_0 < 0; \quad -\infty < q < -1. \end{aligned} \tag{29}$$

The function F is the elliptic integral of the first kind,

$$F(\phi,k) = \int_0^{\phi} \frac{ds}{\sqrt{1-k^2\sin^2 s}}, \tag{30}$$

and

$$\begin{aligned} \cos\alpha &= [1-\sqrt{3}-q(\tau)]/[1+\sqrt{3}-q(\tau)]; \\ & -\infty < q < 1; \quad 0<\alpha<\pi; \quad Q_0 > 0 \\ \cos\gamma &= [1+\sqrt{3}+q(\tau)]/[-1+\sqrt{3}-q(\tau)]; \\ & -\infty < q < -1; \quad 0<\gamma<\pi; \quad Q_0 < 0. \end{aligned} \tag{31}$$

The solution (29) accommodates the sign change indicated in (28) by the fact that the function $q(\tau)$ varies smoothly near $r=0$ for $Q_0>0$ or $Q_0<0$. The elliptic integral, $F(\phi,k)$, is continued beyond $\phi=\pi/2$ using the relation $F(\phi,k) = K + F(\phi-\pi/2,k)$. Later, when we consider the case $Q_0 = 0$, which has a discontinuous first derivative near $r=0$, we will see that the sign change is retained and it is necessary to explicitly distinguish between $r>0$ and $r<0$ cases. For the remainder of the paper the following superscript notation will be used to distinguish various cases of interest:

(i) A quantity valid for $Q_0>0$ will be denoted by a superscript $+$.
(ii) A quantity valid for $Q_0<0$ will be denoted by a superscript $-$.
(iii) A quantity valid for $Q_0=0$ and $r>0$ will be denoted by a superscript $0,>$.
(iv) A quantity valid for $Q_0=0$ and $r<0$ will be denoted by a superscript $0,<$.
(v) A quantity valid for $Q_0=0$ and $r<0$ and $r>0$ will be denoted by a superscript $0,<\ >$.

The relationship between α or γ and $q(\tau)$ in (31) is inverted through the use of Jacobian elliptic functions. We use the cosine amplitude function, cn, defined by $\cos(\phi)\equiv\mathrm{cn}(F) = \mathrm{cn}[(2/3^{1/4})\tau]$. Thus for $Q_0>0$,

$$q^+(\tau) = \frac{(1-\sqrt{3}) - (1+\sqrt{3})\ \mathrm{cn}\{[2/(3)^{1/4}]\tau\}}{1-\mathrm{cn}\{[2/(3)^{1/4}]\tau\}}. \tag{32}$$

The range of variables in (32) is

$$-\infty < q^+ < 1; \quad 0<\tau<[(3)^{1/4}/2]4K = 7.285\,89. \tag{33}$$

The quantity K refers to the complete elliptic integral which for $Q_0>0$ is $K = F[\pi/2, \sin(5\pi/12)] = 2.768\,04$. The result (32) is plotted in Fig. 2(a). Similarly for $Q_0<0$,

$$q^-(\tau) = \frac{-(1+\sqrt{3}) + (1-\sqrt{3})\ \mathrm{cn}\{[2/(3)^{1/4}]\tau\}}{1-\mathrm{cn}\{[2/(3)^{1/4}]\tau\}}, \tag{34}$$

where

$$-\infty < q^- < -1; \quad 0<\tau<[(3)^{1/4}/2]4K = 4.206\,54, \tag{35}$$

and for the case $Q_0<0$, $K = F[\pi/2, \sin(\pi/12)] = 1.598\,14$. The result (34) is plotted in Fig. 2(b).

The functions $r^+(\tau)$ and $r^-(\tau)$ are generated by substituting (32) and (34) into (26) and are also shown in Figs. 2(a) and 2(b).

V. THE CASE $Q_0 = 0$

In this case (23) becomes

$$\begin{aligned} \frac{dq}{d\tau} &= +\frac{2}{\sqrt{3}}(-q^3)^{1/2}; \quad r<0, \\ \frac{dq}{d\tau} &= -\frac{2}{\sqrt{3}}(-q^3)^{1/2}; \quad r>0. \end{aligned} \tag{36}$$

Equation (36) is easily integrated to give, on the left branch, $Q_0=0$, $r<0$,

$$q^{0,<}(\tau) = -\left(\frac{1}{1+(1/\sqrt{3})\tau}\right)^2; \quad 0<\tau<\infty, \tag{37}$$

and on the right branch, $Q_0=0$, $r>0$,

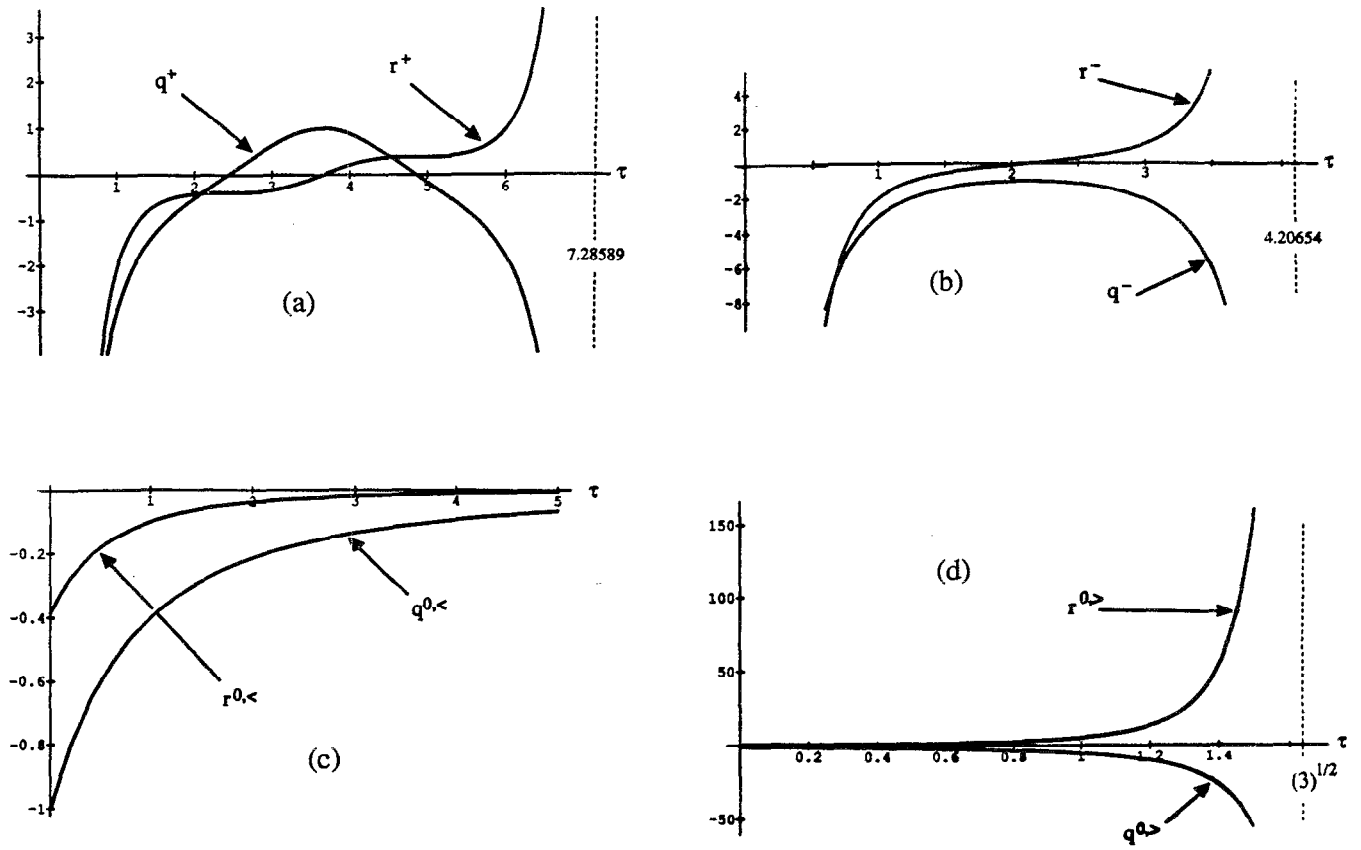

FIG. 2. Temporal behavior of q and r: (a) $Q_0>0$, (b) $Q_0<0$, (c) $Q_0=0, r<0$, and (d) $Q_0=0, r>0$.

$$q^{0,>}(\tau) = -\left(\frac{1}{1-(1/\sqrt{3})\tau}\right)^2; \quad 0<\tau<\sqrt{3}, \tag{38}$$

where it is again noted that variables in (37) and (38) are normalized by $t_0 = 1/(-Q_i)^{1/2}$. The solutions (37) and (38) are shown in Figs. 2(c) and 2(d). Notice that in the case $r>0$ the relation becomes singular when $\tau=(3)^{1/2}$. In all cases, except along the branch $Q_0=0$, $r<0$, the invariants $q(\tau)$ and $r(\tau)$ become singular in a finite time. The corresponding solutions for $r(\tau)$ are

$$r^{0,<}(\tau) = -\frac{2}{3\sqrt{3}}\left(\frac{1}{1+(1/\sqrt{3})\tau}\right)^3; \quad 0<\tau<\infty \tag{39}$$

and

$$r^{0,>}(\tau) = \frac{2}{3\sqrt{3}}\left(\frac{1}{1-(1/\sqrt{3})\tau}\right)^3; \quad 0<\tau<\sqrt{3}, \tag{40}$$

and are also shown in Figs. 2(c) and 2(d).

VI. DETERMINATION OF a_{ij}

We now proceed to the solution of Eq. (25) repeated here for convenience:

$$\frac{d^2a_{ij}}{d\tau^2} + \frac{2}{3}q(\tau)a_{ij} = 0; \quad i,j = 1,2,3. \tag{41}$$

It is convenient to work in terms of the velocity gradient tensor, however, any component of a tensor formed from linear combinations of a_{ij} such as the strain or rotation tensor will also satisfy Eq. (41).

Although (41) appears to be simple, $q(\tau)$ is expressed in terms of elliptic functions and this complicates the determination of exact expressions for $a_{ij}(\tau)$. This problem can be circumvented by noting that $r(\tau)$ is a monotonic function of τ as can be seen in Fig. 2. Rewriting (41) with r as the independent variable leads to

$$\frac{4}{9}\left(\mathrm{sgn}(Q_0) - \frac{27}{4}r^2\right)\frac{d^2a_{ij}}{dr^2} - 4r\frac{da_{ij}}{dr} + \frac{2}{3}a_{ij} = 0, \tag{42}$$

where the dependence of a_{ij} on τ is subsumed in the variable $r(\tau)$. The results in the remainder of this paper will be presented with r as the timelike independent variable. The conversion to actual time can always be accomplished using (32), (34), and (26). The change of variable $s=(3\sqrt{3}/2)r$ puts Eq. (42) into the standard form

$$[\mathrm{sgn}(Q_0) - s^2]\frac{d^2a_{ij}}{ds^2} - \frac{4}{3}s\frac{da_{ij}}{ds} + \frac{2}{9}a_{ij} = 0, \tag{43}$$

which can be solved in terms of hypergeometric functions. The procedure is to convert (43) to a hypergeometric equation using the change of variables $x=1-s^2$ for the case $Q_0>0$ and $x=1+s^2$ for the case $Q_0<0$. The hypergeometric functions of interest are ${}_2F_1(a,b,c;z)$ where ${}_2F_1$ is a single valued function in the complex z plane with a cut along

the real axis from 1 to $+\infty$. Actually the solution expressed in the form of a hypergeometric series is not particularly useful and to make progress it is essential to relate the series to well-known functions. The functions of interest are as follows:

$$ {}_2F_1\left(\frac{1}{6},-\frac{1}{6},\frac{1}{2};\frac{1}{z}\right)=\cos\left[\frac{1}{3}\sin^{-1}\left(\frac{1}{(z)^{1/2}}\right)\right] $$

and

$$ {}_2F_1\left(\frac{2}{3},\frac{1}{3},\frac{3}{2};\frac{1}{z}\right)=3z^{1/2}\sin\left[\frac{1}{3}\sin^{-1}\left(\frac{1}{(z)^{1/2}}\right)\right] $$

for $Q_0>0$ and

$$ {}_2F_1\left(\frac{1}{6},\frac{2}{3},\frac{4}{3};z\right)=2^{1/3}[1+(1-z)^{1/2}]^{-1/3} $$

and

$$ {}_2F_1\left(-\frac{1}{6},\frac{1}{3},\frac{2}{3};z\right)=2^{-1/3}[1+(1-z)^{1/2}]^{1/3} $$

for $Q_0<0$ (see Abramowitz and Stegun,[11] p. 558, items 15.1.1, 15.1.13, 15.1.15, and 15.1.17). All three cases of interest are expressed in terms of simple functions. Solutions of (42) are of the form

$$ a_{ij}(r)=C_{ij}f_1(r)+D_{ij}f_2(r), \tag{44} $$

where f_1 is an even function of r and f_2 is odd and C_{ij} and D_{ij} are matrix constants of integration determined by initial conditions. It is customary to normalize f_1 and f_2 such that

$$ f_1(0)=1,\quad \left(\frac{df_1}{dr}\right)_{r=0}=0,\quad f_2(0)=0,\quad \left(\frac{df_2}{dr}\right)_{r=0}=1, \tag{45} $$

and this normalization will be used here although it will ordinarily not be the case that the problem is initiated at $r=0$.

The result for $Q_0>0$ is

$$ f_1^+(r)=\frac{1}{2}\left[\left(1+\frac{3\sqrt{3}}{2}r\right)^{1/3}+\left(1-\frac{3\sqrt{3}}{2}r\right)^{1/3}\right] \tag{46} $$

and

$$ f_2^+(r)=\frac{1}{\sqrt{3}}\left[\left(1+\frac{3\sqrt{3}}{2}r\right)^{1/3}-\left(1-\frac{3\sqrt{3}}{2}r\right)^{1/3}\right]. \tag{47} $$

The solutions (46) and (47) are plotted in Figs. 3(a) and 3(b). A number of expressions in this paper would be simplified by working entirely in terms of s going all the way back to Eq. (17). Unfortunately, this would deviate from a widely accepted form of the third invariant defined essentially by Eq. (9). For this reason the factor $3\sqrt{3}/2$ in front of r will be carried along in spite of the inconvenience. At least it can serve as a reminder that the properties of a cubic equation provide the underlying framework of the problem. For $Q_0<0$

$$ f_1^-(r)=(1+\tfrac{27}{4}r^2)^{1/6}\cos\{\tfrac{1}{3}\tan^{-1}[(3\sqrt{3}/2)r]\} \tag{48} $$

and

$$ f_2^-(r)=(2/\sqrt{3})(1+\tfrac{27}{4}r^2)^{1/6}\sin\{\tfrac{1}{3}\tan^{-1}[(3\sqrt{3}/2)r]\}. \tag{49} $$

See Figs. 3(c) and 3(d). Finally for $Q_0=0$,

$$ f_1^{0,<>}(r)=2^{1/3}[(3\sqrt{3}/2)r]^{-2/3} \tag{50} $$

and

$$ f_2^{0,<>}(r)=(2^{2/3}/3\sqrt{3})[(3\sqrt{3}/2)r]^{1/3}. \tag{51} $$

The results (50) and (51) are valid for both positive and negative values of r as long as the appropriate function of time [either (39) or (40)] is used. The solutions (50) and (51) are plotted in Figs. 3(e) and 3(f). It turns out that the normalization (45) generates the Wronskian

$$ f_1(r)\left(\frac{df_2}{dr}\right)-\left(\frac{df_1}{dr}\right)f_2(r)=\frac{1}{[q(r)]^2} $$

for all three cases.

VII. RATE OF STRAIN AND RATE OF ROTATION TENSORS

The discussion cannot be completed without some consideration of the behavior of the straining and rotational parts of the motion. In dimensionless form Eq. (6) is

$$ \frac{da_{ij}}{d\tau}+a_{ik}a_{kj}+\frac{2}{3}q\delta_{ij}=0. \tag{52} $$

The velocity gradient tensor is decomposed into a symmetric and antisymmetric part

$$ a_{ij}=\tfrac{1}{2}(a_{ij}+a_{ji})+\tfrac{1}{2}(a_{ij}-a_{ji})=s_{ij}+w_{ij}, \tag{53} $$

where s_{ij} and w_{ij} are the strain-rate and rotation-rate tensors, respectively. The invariants of the velocity gradient tensor can be written in terms of the invariants of the strain-rate and rotation-rate tensors as

$$ \begin{aligned} q&=-\tfrac{1}{2}a_{im}a_{mi}=q_s+q_w,\\ r&=r_s-w_{im}w_{mk}s_{ki}, \end{aligned} \tag{54} $$

where

$$ \begin{aligned} q_s&=-\tfrac{1}{2}s_{im}s_{mi},\\ q_w&=-\tfrac{1}{2}w_{im}w_{mi}=\omega_i\omega_i,\\ r_s&=-\tfrac{1}{3}s_{im}s_{mk}s_{ki}. \end{aligned} \tag{55} $$

The quantity ω_i is a component of the vorticity vector and the relation $w_{ij}=e_{ijk}\omega_k$ has been used where e_{ijk} is the Levi-Civita tensor. The quantity q_w is usually called the enstrophy. Equation (52) can be used to generate transport equations for the rate-of-strain tensor s_{ij}, and rate-of-rotation tensor w_{ij}. These are

$$ \frac{d}{d\tau}(s_{ij})+s_{ik}s_{kj}+w_{ik}w_{kj}+\frac{2}{3}q\delta_{ij}=0, \tag{56} $$

or in terms of the vorticity vector,

$$ \frac{d}{d\tau}(s_{ij})+s_{ik}s_{kj}+\omega_i\omega_j+\left(\frac{2}{3}q-q_w\right)\delta_{ij}=0 \tag{57} $$

and

$$ \frac{d}{d\tau}(w_{ij})+w_{ik}s_{kj}+s_{ik}w_{kj}=0 \tag{58} $$

or

$$ \frac{d}{d\tau}(\omega_i)-\omega_k s_{ki}=0. \tag{59} $$

Equation (59) is used to generate an evolution equation for the enstrophy

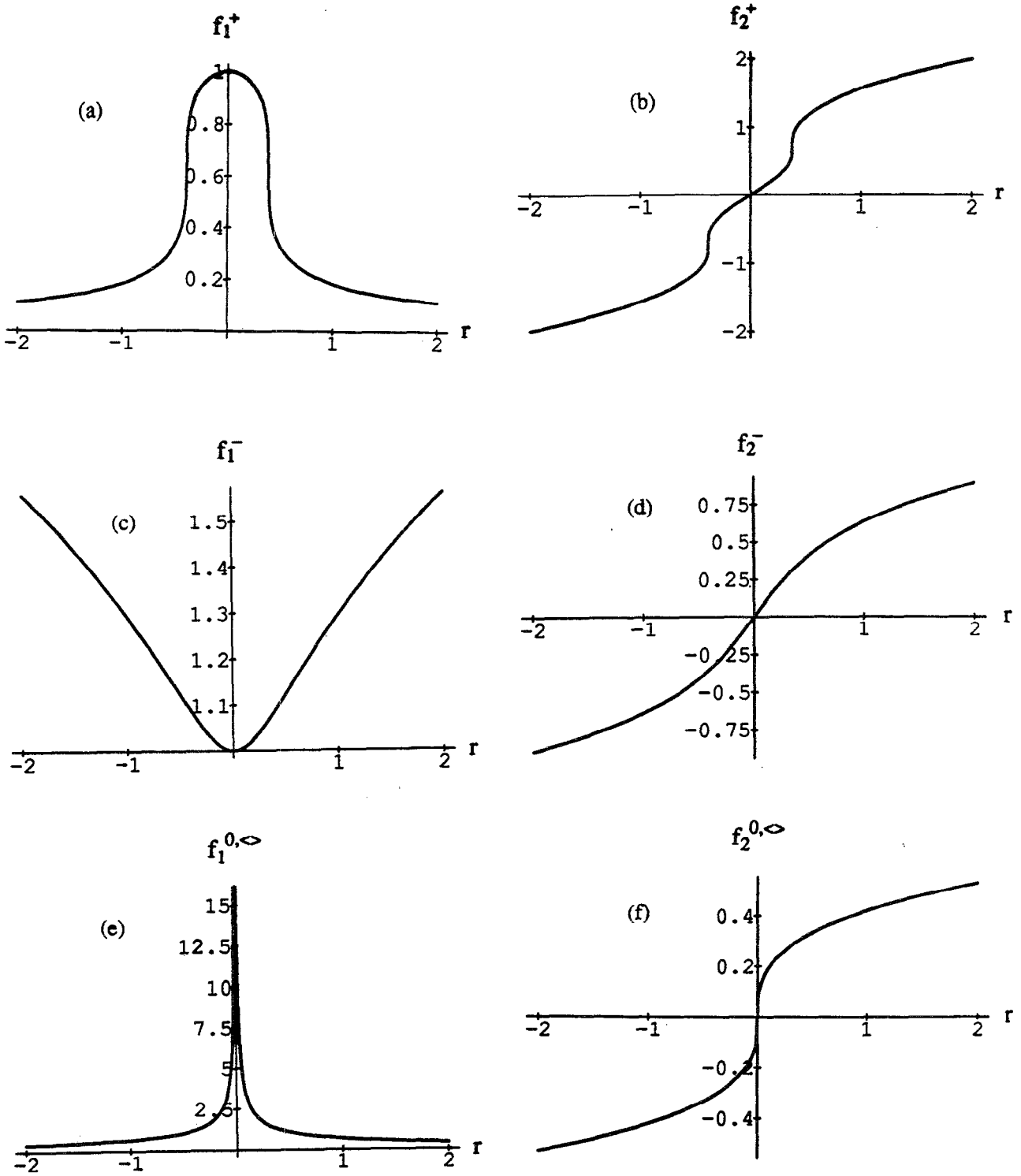

FIG. 3. Solution functions with independent variable r: (a) $Q_0 > 0$ even, (b) $Q_0 > 0$ odd, (c) $Q_0 < 0$ even, (d) $Q_0 < 0$ odd, (e) $Q_0 = 0$ even, (f) $Q_0 = 0$ odd.

$$\frac{dq_w}{d\tau} = 2\omega_i \omega_k s_{ki} = 2(r_s - r). \tag{60}$$

Once $q(\tau)$, $r(\tau)$ $q_w(\tau)$, and $d\,q_w/d\tau$ are known, the evolution of the strain invariants q_s and r_s is determined using (54) and (60).

VIII. INITIAL CONDITIONS

The exact solution determined in Sec. VI permits a direct connection to be made between the initial conditions of the velocity gradient field and the asymptotic behavior of the solution. Equation (43) defines a simple, linear initial value

problem and normally the constants C_{ij} and D_{ij} would be determined by independently specifying the function a_{ij} and its derivative with respect to r (or τ) at some initial time. Our case differs from the usual situation in that a specification of the initial value of a_{ij} also specifies the initial time derivative through Eq. (52). The constants of integration are given by

$$C_{ij} = \frac{\hat{a}_{ij}(df_2/dr)_{\hat{r}} - (\hat{da}_{ij}/dr)f_2(\hat{r})}{f_1(\hat{r})(df_2/dr)_{\hat{r}} - (df_1/dr)_{\hat{r}}f_2(\hat{r})}$$
$$= \hat{a}_{ij}[q(\hat{r})]^2\left(\frac{df_2}{dr}\right)_{\hat{r}} + \left(\frac{3}{2}(\hat{a}_{ik}\hat{a}_{kj}) + q(\hat{r})\delta_{ij}\right)f_2(\hat{r}), \tag{61}$$

$$D_{ij} = \frac{(\hat{da}_{ij}/dr)f_1(\hat{r}) - \hat{a}_{ij}(df_1/dr)_{\hat{r}}}{f_1(\hat{r})(df_2/dr)_{\hat{r}} - (df_1/dr)_{\hat{r}}f_2(\hat{r})}$$
$$= -\hat{a}_{ij}[q(\hat{r})]^2\left(\frac{df_1}{dr}\right)_{\hat{r}}$$
$$-\left(\frac{3}{2}(\hat{a}_{ik}\hat{a}_{kj}) + q(\hat{r})\delta_{ij}\right)f_1(\hat{r}), \tag{62}$$

where $\hat{r}$ is the initial value of r, $\hat{a}_{ij}$ refers to chosen initial values of the components of a_{ij}, and $\hat{da}_{ij}/dr$ is the corresponding initial derivative computed from

$$\frac{\hat{da}_{ij}}{dr} = -\frac{1}{[q(\hat{r})]^2}\left(\frac{3}{2}(\hat{a}_{ik}\hat{a}_{kj}) + q(\hat{r})\delta_{ij}\right). \tag{63}$$

Using (63) and the given initial values $\hat{a}_{ij}$, the constants C_{ij} and D_{ij} are exactly defined.

Not only is the initial time derivative set by the choice of $\hat{a}_{ij}$ but so too is the initial time! This comes about as follows. First, values of $\hat{A}_{ij}$ are specified. This determines initial values of Q and R and the characteristic time parameter Q_0 through Eq. (17). This in turn fixes the initial value $\hat{q}$, and, through (29), the initial dimensionless time $\hat{\tau}$, which will lie in one of the ranges (33) or (35). The system then evolves from this state according to (32), (34), (37) or (38) and (44)–(51) depending on Q_0. The fact that $\hat{\tau}$ is predetermined is not inconsistent with, say, a numerical solution of (6) which begins at $t=0$ since the functions q and r can always be shifted by a constant phase.

IX. UNIVERSAL STRUCTURE OF C_{ij} AND D_{ij}

The problem being considered is somewhat unusual in that the solution (44) of the linear second-order problem (41) must also satisfy the original, nonlinear, first-order system (52). The nonlinearity of (52) places certain restrictions on C_{ij} and D_{ij} which we shall now explore. First rewrite (52) with time replaced by r,

$$\frac{2}{3}\left(\mathrm{sgn}(Q_0) - \frac{27}{4}r^2\right)^{2/3}\frac{da_{ij}}{dr} + a_{ik}a_{kj}$$
$$+\frac{2}{3}\left(\mathrm{sgn}(Q_0) - \frac{27}{4}r^2\right)^{1/3}\delta_{ij} = 0. \tag{64}$$

Substituting (44),

$$\frac{2}{3}\left(\mathrm{sgn}(Q_0) - \frac{27}{4}r^2\right)^{2/3}\left(C_{ij}\frac{df_1(r)}{dr} + D_{ij}\frac{df_2(r)}{dr}\right)$$
$$+[C_{ik}f_1(r) + D_{ik}f_2(r)][C_{kj}f_1(r) + D_{kj}f_2(r)]$$
$$+\frac{2}{3}\left(\mathrm{sgn}(Q_0) - \frac{27}{4}r^2\right)^{1/3}\delta_{ij} = 0. \tag{65}$$

The various solutions for $f_1(r)$ and $f_2(r)$, (46)–(51), are substituted in turn into (65). When this is done the resulting expression for each case can be sorted into three groups corresponding to three independent functions. The coefficients of these functions involve various combinations of C_{ij} and D_{ij} that must equal zero. The case $Q_0 = 0$ is the simplest and can be used to illustrate the procedure. Substitute (50) and (51) into (65) to give

$$4r^{-4/3}(C_{ik}C_{kj}) + 2^{-1/3}r^{2/3}$$
$$\times[2D_{ik}D_{kj} + 3(2)^{1/3}D_{ij} - 9(2)^{2/3}\delta_{ij}]$$
$$+2^{4/3}r^{-1/3}[D_{ik}C_{kj} + C_{ik}D_{kj} - 3(2)^{1/3}C_{ij}] = 0. \tag{66}$$

In order for Eq. (66) to be satisfied for all r, the coefficients of each of the independent functions of r must be zero. A similar equation can be generated for each of the other two cases leading to similar conditions on the initial condition matrices C_{ij} and D_{ij}. These have been determined as follows.

Case 1—$Q_0 > 0$:

$$3C^+_{ik}C^+_{kj} - 4D^+_{ik}D^+_{kj} + 4\delta_{ij} = 0, \tag{67}$$
$$2D^+_{ik}D^+_{kj} + D^+_{ij} - \delta_{ij} = 0, \tag{68}$$
$$D^+_{ik}C^+_{kj} + C^+_{ik}D^+_{kj} - C^+_{ij} = 0, \tag{69}$$

with invariants $(P_{C^+}, Q_{C^+}, R_{C^+}) = (0,1,0)$ and $(P_{D^+}, Q_{D^+}, R_{D^+}) = (0, -\frac{3}{4}, \frac{1}{4})$ [cf. the definitions of P, Q, and R in (11)].

Case 2—$Q_0 < 0$:

$$3C^-_{ik}C^-_{kj} + 4D^-_{ik}D^-_{kj} - 4\delta_{ij} = 0, \tag{70}$$
$$2D^-_{ik}D^-_{kj} - D^-_{ij} - \delta_{ij} = 0, \tag{71}$$
$$D^-_{ik}C^-_{kj} + C^-_{ik}D^-_{kj} + C^-_{ij} = 0, \tag{72}$$

with invariants $(P_{C^-}, Q_{C^-}, R_{C^-}) = (0, -1, 0)$ and $(P_{D^-}, Q_{D^-}, R_{D^-}) = (0, -\frac{3}{4}, \frac{1}{4})$.

Case 3—$Q_0 = 0$:

$$C^0_{ik}C^0_{kj} = 0, \tag{73}$$
$$2D^0_{ik}D^0_{kj} + 3(2)^{1/3}D^0_{ij} - 9(2)^{2/3}\delta_{ij} = 0, \tag{74}$$
$$D^0_{ik}C^0_{kj} + C^0_{ik}D^0_{kj} - 3(2)^{1/3}C^0_{ij} = 0, \tag{75}$$

with invariants $(P_{C^0}, Q_{C^0}, R_{C^0}) = (0,0,0)$ and $(P_{D^0}, Q_{D^0}, R_{D^0}) = [0, -27/(2)^{4/3}, \frac{27}{2}]$.

The values of the invariants are generated by making use of the Cayley–Hamilton theorem and taking the appropriate traces in the above relationships. It can be easily shown that, in all cases, the matrices C_{ij} and D_{ij} commute.

It is important to recognize that the relations (67)–(75) are not imposed on the problem but are automatically satisfied by any set of C_{ij} and D_{ij} generated by (61) and (62). Thus, even though the choice of initial values of A_{ij} is completely arbitrary subject to the incompressibility condition, the associated matrices C_{ij} and D_{ij} generated from (61) and (62) are not arbitrary. This is a consequence of the basic

nonlinearity of the system and the fact that an initial choice of A_{ij} has associated with it a particular initial value $\hat{r}$ that in turn dictates the action of the solution functions f_1 and f_2 which appear in (61) and (62). In contrast to a simple linear system, the coefficients and function values in (61) and (62) are coupled and this coupling generates solution matrices C_{ij} and D_{ij} which have a universal structure.

X. ASYMPTOTIC BEHAVIOR OF THE VORTICITY AND RATE OF STRAIN

The results of the previous section can be used to provide a detailed description of the asymptotic behavior of the velocity gradient tensor. Here it is necessary to distinguish four cases: $Q_0>0$; $Q_0<0$; $Q_0=0,r>0$; and $Q_0=0,r<0$. The first three behave as

$$\lim_{r\to\infty} a_{ij}^{+}(r) = (2^{2/3}D_{ij}^{+})r^{1/3},$$

$$\lim_{r\to\infty} a_{ij}^{-}(r) = [(3/2^{4/3})C_{ij}^{-} + (1/2^{1/3})D_{ij}^{-}]r^{1/3}, \tag{76}$$

$$\lim_{r\to\infty} a_{ij}^{0,>}(r) = [(2^{1/3}/3)D_{ij}^{0,>}]r^{1/3}.$$

All three cases become singular as the system evolves toward the maximum time. At first sight it would appear from (76) that the geometry of the limiting solution could be quite different depending on whether Q_0 is positive, negative, or zero and depending on the detailed structure of the matrices C_{ij} and D_{ij}. However, it was seen in the previous section that certain properties of these matrices are universal. That is the issue we want to now explore. What aspects of the asymptotic behavior are universal and what information from the initial specification of A_{ij} penetrates to the asymptotic state?

The asymptotic limit for the left branch $Q_0=0,r<0$ which evolves for infinite time is

$$\lim_{r\to 0} a_{ij}^{0,<}(r) = (\tfrac{2}{3}C_{ij}^{0,<})r^{-2/3}. \tag{77}$$

Even though Q and R go to zero for this case, the individual components of the velocity gradient tensor still become singular. The evolution of the invariants of the strain and rotation tensors can be easily determined from (54) and (55) and nothing further will be said about this case.

The algebraic equations governing C_{ij} and D_{ij} may be used to explore (76) more fully. Equation (74) is an uncoupled equation for the components of $(2^{1/3}/3)D_{ij}^{0,>}$. Equations (70)–(72) can be rearranged to construct an equation for the sum $(3/2^{4/3})C_{ij}^{-} + (1/2^{1/3})D_{ij}^{-}$, which is identical to (74). Similarly, (68) can be rearranged to form the same equation for $2^{2/3}D_{ij}^{+}$. So the asymptotic behavior of all three cases in (76) is completely described by solutions of the generic equation

$$K_{ik}K_{kj} + (1/2^{1/3})K_{ij} - 2^{1/3}\delta_{ij} = 0, \tag{78}$$

where $K_{ij} = 2^{2/3}D_{ij}^{+}$ if $Q_0>0$, $K_{ij} = (3/2^{4/3})C_{ij}^{-} + (1/2^{1/3})D_{ij}^{-}$ if $Q_0<0$, and $K_{ij} = (2^{1/3}/3)D_{ij}^{0,>}$ if $Q_0=0$. The invariants of K_{ij} are $(P_K,Q_K,R_K) = (0,-3/2^{2/3},1)$ which lies on the boundary (18). Thus the eigenvalues of K_{ij} are real with two equal. The result (78) can also be easily obtained by substituting

$$\lim_{r\to\infty} a_{ij}(r) = K_{ij}r^{1/3} \tag{79}$$

into (64). In the limit $r\to\infty$

$$\frac{3}{2^{1/3}}r^{4/3}\frac{da_{ij}}{dr} + a_{ik}a_{kj} - 2^{1/3}r^{2/3}\delta_{ij} = r^{2/3}\left(K_{ik}K_{kj} + \frac{1}{2^{1/3}}K_{ij} - 2^{1/3}\delta_{ij}\right) = 0. \tag{80}$$

The matrix K_{ij} can be decomposed into a symmetric and an antisymmetric part

$$K_{ij} = S_{ij} + W_{ij}. \tag{81}$$

The matrices S_{ij} and W_{ij} will be referred to as the asymptotic rate of strain and rate of rotation although they differ from the true asymptotic rates by a factor of $r^{1/3}$. Substituting (81) into (78) and transforming to coordinates aligned with the principal axes of S_{ij} so that

$$K_{ij} = \begin{bmatrix} S_{11} & \Omega_3 & -\Omega_2 \\ -\Omega_3 & S_{22} & \Omega_1 \\ \Omega_2 & -\Omega_1 & -S_{11}-S_{22} \end{bmatrix}, \tag{82}$$

leads to the following independent algebraic relations for the components of K_{ij}:

$$\Omega_1\Omega_2 = \Omega_1\Omega_3 = \Omega_2\Omega_3 = 0, \tag{83}$$

$$\left(-\frac{1}{2^{1/3}} + S_{11}\right)\Omega_1 = \left(-\frac{1}{2^{1/3}} + S_{22}\right)\Omega_2 = \left(\frac{1}{2^{1/3}} + \frac{1}{2}S_{11} + \frac{1}{2}S_{22}\right)\Omega_3 = 0, \tag{84}$$

$$-2^{1/3} + (1/2^{1/3})S_{11} + S_{11}^2 - (\Omega_2^2+\Omega_3^2) = -2^{1/3} + (1/2^{1/3})S_{22} + S_{22}^2 - (\Omega_1^2+\Omega_3^2) = 0, \tag{85}$$

$$-2^{1/3} - (1/2^{1/3})(S_{11}+S_{22}) + (S_{11}+S_{22})^2 - (\Omega_1^2+\Omega_2^2) = 0, \tag{86}$$

where Ω_1, Ω_2, and Ω_3 are the components of W_{ij} referred to principal axes of strain and S_{11} and S_{22} are the principal strains. From (83) we see that we need only consider two possible cases, either all components of the vorticity are zero or any two are zero. In the case where all three components are zero the principal rates of strain determined from (85) and (86) are uniquely determined

$$(S_{11},S_{22},S_{33}) = \left(\frac{1}{2^{1/3}},\frac{1}{2^{1/3}},-\frac{2}{2^{1/3}}\right).$$

In the case where one vorticity component is nonzero, say Ω_1, then $S_{11} = 1/2^{1/3}$ and

$$\Omega_1^2 = S_{22}^2 + (1/2^{1/3})S_{22} - 2^{1/3}. \tag{87}$$

The positivity of Ω_1^2 requires that $S_{22} > 1/2^{1/3}$. *Thus the asymptotic configuration in principal axes of strain is one with two positive strain rates and the vorticity exactly aligned with the intermediate positive strain.* Moreover, for S_{22} somewhat larger than $1/2^{1/3}$ Eq. (87) is approximately $\Omega_1^2 \approx S_{22}^2$. Equation (87) is equivalent to the result

$$Q_{W_K} = -\tfrac{1}{2}W_{ik}W_{ki} = \Omega_i\Omega_i - Q_{S_K} - (3/2^{2/3}), \tag{88}$$

which can be generated directly from (78) [cf. the invariant definitions in (11)]. All of these features just discussed are observed in the studies of Chen *et al.*[8] and Sondergaard *et al.*[9] when the observations are conditioned on regions of high dissipation. Similar relations for the other invariants of S_{ij} and W_{ij} can be generated as

$$R_{S_K} = (1/2^{1/3})Q_{W_K} + 1 \tag{89}$$

and

$$W_{ik}W_{kn}W_{ni} = R_{S_K} - R_K = (1/2^{1/3})Q_{W_K}. \tag{90}$$

The geometry of the asymptotic state is completely determined by Q_{W_K} a single scalar function of initial conditions.

XI. EXPLICIT CONNECTION BETWEEN THE ASYMPTOTIC STATE AND INITIAL CONDITIONS

It was noted by Chen *et al.*[7] that, in direct simulations of a time developing mixing layer in the neighborhood of regions of high dissipation, that the second and third invariants of the rate-of-strain tensor were related by

$$q_s/(\tfrac{27}{4}r_s^2)^{1/3} = -k, \tag{91}$$

where k is a constant that appears to be independent of initial conditions equal to approximately 1.4. This corresponds closely to the 3, 1, -4 ratio of principal strains observed in homogeneous turbulence by Ashurst *et al.*[3] The asymptotic behavior of the present model gives

$$\lim_{r\to\infty} \frac{q_s}{(\frac{27}{4}r_s^2)^{1/3}} = -\frac{[(2^{2/3}/3)Q_{W_K}+1]}{[(1/2^{1/3})Q_{W_K}+1]^{2/3}}. \tag{92}$$

In this case the ratio is connected to the initial conditions through the quantity Q_{W_K}. Equation (92) is shown plotted in Fig. 4 which indicates that relatively large values of Q_{W_K} on the order of ten or so are required to reproduce the observed value of k. To explore this further we return to (61) and (62) and write an equation for K_{ij}:

$$K_{ij} = -\hat{a}_{ij}\hat{q}^2\frac{\hat{dg}}{dr} - \left(\frac{3}{2}(\hat{a}_{ik}\hat{a}_{kj}) + \hat{q}\delta_{ij}\right)\hat{g}, \tag{93}$$

with the antisymmetric part (not necessarily resolved in principal axes of strain) given by

$$\Omega_i = -\hat{\omega}_i\left(\hat{q}^2\frac{\hat{dg}}{dr}\right) + \hat{\omega}_k\hat{s}_{ki}\left(\frac{3}{2}\hat{g}\right), \tag{94}$$

where the " ^ " denotes an initial value and

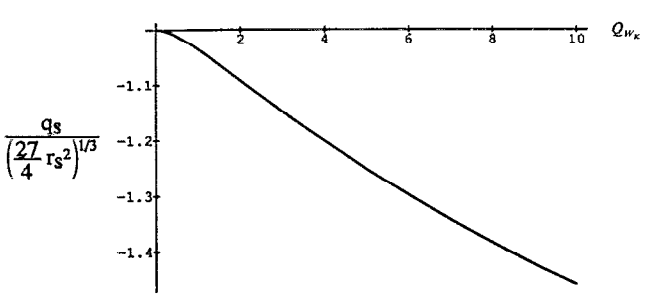

FIG. 4. Dependence of asymptotic strain invariants on asymptotic vorticity.

$$g^+ = 2^{2/3}f_1^+, \quad g^- = \frac{1}{2^{1/3}}\left(f_1^- - \frac{3}{2}f_2^-\right),$$

$$g^{0,>} = \frac{2^{1/3}}{3}f_1^{0,>}. \tag{95}$$

Substituting (95) into (94) and using (46)–(51) leads to the following expressions for the asymptotic vorticity:

$$\Omega_i^+ = (3/2^{1/3})\hat{f}_1^+(\hat{f}_2^+\hat{\omega}_i + \hat{\omega}_k\hat{s}_{ki}), \tag{96}$$

$$\Omega_i^{0,>} = (1/2^{2/3})\hat{f}_1^{0,>}[3(2)^{1/3}\hat{f}_2^{0,>}\hat{\omega}_i + \hat{\omega}_k\hat{s}_{ki}], \tag{97}$$

and

$$\Omega_i^- = \frac{3}{2^{4/3}}\left\{\hat{\omega}_i\frac{1}{\hat{q}}\left[\left(\hat{f}_1^- + \frac{1}{2}\hat{f}_2^-\right) - \frac{3}{2}r\left(\hat{f}_1^- - \frac{3}{2}\hat{f}_2^-\right)\right] + \hat{\omega}_k\hat{s}_{ki}\left(\hat{f}_1^- - \frac{3}{2}\hat{f}_2^-\right)\right\}. \tag{98}$$

Using (96)–(98) Q_{W_K} can be written in terms of the initial components of the vorticity vector and rate of strain as

$$Q_{W_K}^+ = (9/2^{2/3})(\hat{f}_1^+)^2[(\hat{f}_2^+)^2\hat{\omega}_i\hat{\omega}_i + (2\hat{f}_2^+)\hat{\omega}_i\hat{\omega}_k\hat{s}_{ki} + \hat{\omega}_i\hat{\omega}_n\hat{s}_{nk}\hat{s}_{ki}], \tag{99}$$

$$Q_{W_K}^{0,>} = (1/2^{4/3})(\hat{f}_1^{0,>})^2\{9(2)^{2/3}(\hat{f}_2^{0,>})^2\hat{\omega}_i\hat{\omega}_i + [6(2)^{1/3}\hat{f}_2^{0,>}]\hat{\omega}_i\hat{\omega}_k\hat{s}_{ki} + \hat{\omega}_i\hat{\omega}_n\hat{s}_{nk}\hat{s}_{ki}\}, \tag{100}$$

and

$$Q_{W_K}^- = \frac{9}{4(2)^{2/3}}\left\{\frac{1}{\hat{q}^2}\left[\left(\hat{f}_1^- + \frac{1}{2}\hat{f}_2^-\right) - \frac{3}{2}r\left(\hat{f}_1^- - \frac{3}{2}\hat{f}_2^-\right)\right]^2\hat{\omega}_i\hat{\omega}_i + \frac{2}{\hat{q}}\left[\left(\hat{f}_1^- + \frac{1}{2}\hat{f}_2^-\right) - \frac{3}{2}r\left(\hat{f}_1^- - \frac{3}{2}\hat{f}_2^-\right)\right]\left(\hat{f}_1^- - \frac{3}{2}\hat{f}_2^-\right)\hat{\omega}_i\hat{\omega}_k\hat{s}_{ki} + \left(\hat{f}_1^- - \frac{3}{2}\hat{f}_2^-\right)^2\hat{\omega}_i\hat{\omega}_n\hat{s}_{nk}\hat{s}_{ki}\right\}. \tag{101}$$

The magnitude of Ω_i determines the enstrophy of the final state and, through relations (88) and (89), the complete topological state of the asymptotic solution. The asymptotic state for any given set of initial conditions is now easily determined.

Figure 5 shows four representative cases for increasing values of Q_{W_K}. The dashed lines in these figures represent the three branches of the solution shown in Fig. 1(b) and the boxed quantities are the dimensioned initial values of the velocity gradient tensor referred to initial principal axes of strain. The value of the asymptotic vorticity divided by $r^{2/3}$, Q_{W_K}, computed from (99)–(101), is also shown boxed. The evolution of the flow is depicted in the left-hand plot as a function of r and in the right-hand plot q_s is shown as a function of r_s. For each curve the initial condition is indicated in the form of a solid dot.

In Fig. 5(a) the flow is initially in a state of pure rotation. This leads to initial values $\hat{r} = 0, f_1^+(\hat{r}) = 0$ and from (99) it can be seen that the asymptotic vorticity must decay to zero. As the vorticity decays the strain rate grows and the flow eventually evolves to a state of axisymmetric strain. In Fig. 5(b) the flow is initiated as a state of plain strain with

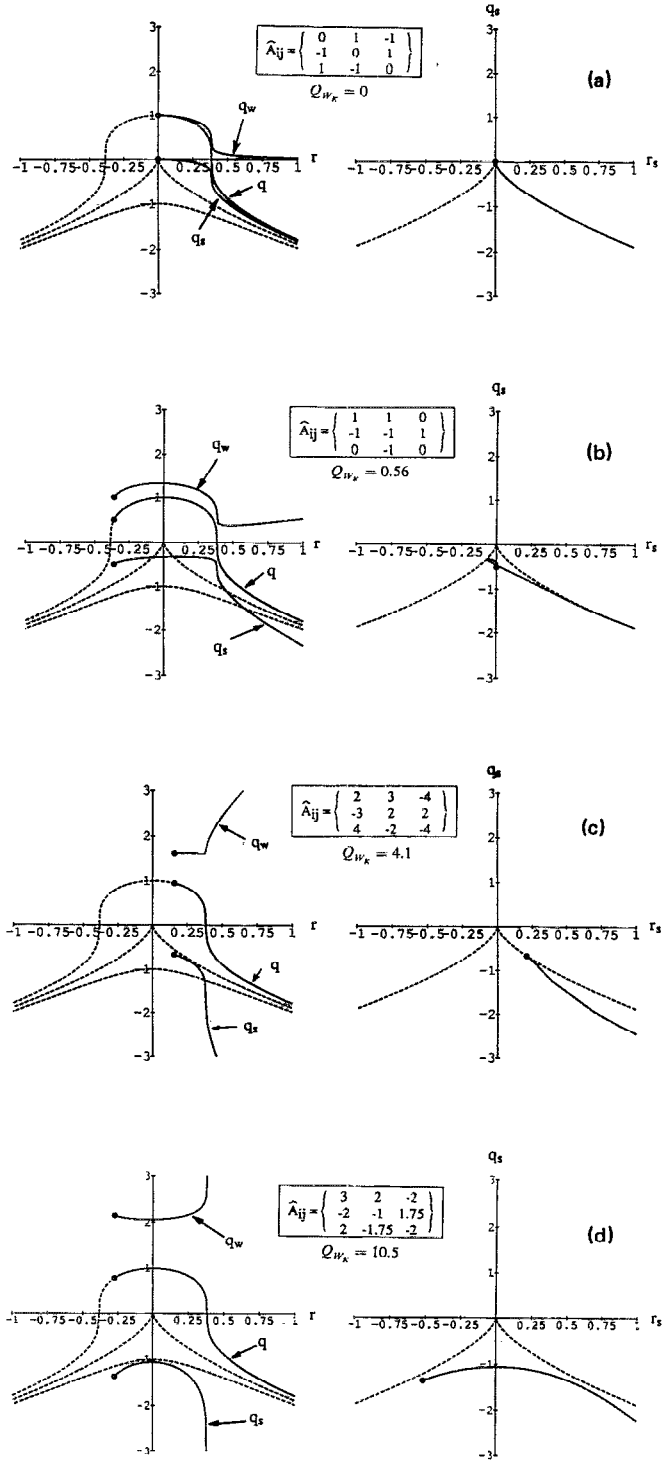

FIG. 5. Evolution of tensor invariants for several selected initial conditions.

two nonzero components of vorticity. In this case the vorticity first grows, then decays, and then grows asymptotically with $Q_{W_K} = 0.56$. The strain invariants execute a small loop and then approach the boundary (18). The value of Q_{W_K} is relatively small and from Eq. (92) and Fig. 4 one can conclude that the asymptotic strain invariants will fall just slightly below the dashed boundary in the right-hand plot in Fig. 5(b). Indeed the difference is indistinguishable in this figure. In Fig. 5(c) the flow is initiated in a state of axisymmetric compression with all three vorticity components nonzero. The asymptotic vorticity grows rapidly and the strain invariants asymptote to a nonaxisymmetric state with two positive strains and one negative strain.

Figure 5(d) shows a case where the initial conditions are chosen to generate an asymptotic state which approximates that observed in simulations ($Q_{W_K} = 10.5$). The flow begins in a state with two negative and one positive principal strains and all three components of the vorticity nonzero. In all the cases depicted in Fig. 5, the asymptotic state is approached rather quickly with the qualitative behavior of the asymptotic solution apparent by the time r has reached one.

XII. CONCLUSIONS

To a large degree the exact theory presented here confirms the results of the asymptotic analysis of Vieillefosse. The main new results are the solutions (32), (34), and (46)–(51) and the treatment of the initial conditions in Secs. IX and X culminating in the matrix equation (78) which defines the universal features of the asymptotic state. It is seen that for any initial condition other than $R<0$, $Q_0 = 0$ the velocity gradient tensor evolves to a geometry with two positive principal rates of strain and the vorticity aligned with the intermediate positive strain rate. This result is interesting in that it suggests that, in spite of all the objections which can be raised against the assumption $H_{ij} = 0$, this case may in fact provide a useful model of some aspects of the mechanism by which the geometry of fine-scale motions in turbulence can evolve to a universal state. The close correspondence between the geometry predicted by the theory and the geometry observed in direct numerical simulations adds support to this conclusion. What is still entirely open is the question of how the balance of terms implied by (6) can have any relevance at all to real flows and at what scale of motion it might apply. It cannot apply at large scales where pressure-driven eddy interactions are important and it would not be expected to apply at the smallest scales where viscosity is important and where the velocity gradients are limited by viscous diffusion. Indeed for all typical free shear flows the gradients associated with turbulent microscales *decrease* with time when referred to a Lagrangian observer. The only option left where (6) might apply is the inertial subrange. Somehow the relatively inviscid motions of the inertial subrange must be matched to the strongly viscous motions at the Kolmogorov microscale in a way that leaves the basic geometry of the flow invariant. To establish how this might occur, much more information is required in a variety of flows of the source term H_{ij} and associated products with A_{ij} which arise in (12), (13), and (16).

ACKNOWLEDGMENT

This work was supported by the Office of Naval Research under Grant No. N00014-90-J-1976-P00001. The burden of solution checking was eased considerably through the use of MATHEMATICA 1.2.1.

[1] P. Vieillefosse, "Local interaction between vorticity and shear in a perfect incompressible fluid," J. Phys. (Paris) **43**, 837 (1982).
[2] P. Vieillefosse, "Internal motion of a small element of fluid in an inviscid flow," Physica A **125**, 150 (1984).
[3] W. T. Ashurst, A. R. Kerstein, R. M. Kerr, and C. H. Gibson, "Alignment of vorticity and scalar gradient with strain rate in simulated Navier–Stokes turbulence," Phys. Fluids **30**, 2343 (1987).
[4] A. Vincent and M. Menguzzi, "The spatial structure and statistical properties of homogeneous turbulence," J. Fluid Mech. **225**, 1 (1991).
[5] G. R. Ruetsch and M. R. Maxey, "Small-scale features of vorticity and passive scalar fields in homogeneous isotropic turbulence," Phys. Fluids A **3**, 1587 (1991).
[6] A. Pumir and E. Siggia, "Collapsing solutions to the 3-D Euler equations," Phys. Fluids A **2**, 220 (1990).
[7] S. S. Girimaji and S. B. Pope, "A diffusion model for velocity gradients in turbulence," Phys. Fluids A **2**, 220 (1990).
[8] J. H. Chen, M. S. Chong, J. Soria, R. Sondergaard, A. E. Perry, M. Rogers, R. Moser, and B. J. Cantwell, "A study of the topology of dissipating motions in direct numerical simulations of time developing compressible and incompressible mixing layers," *Center for Turbulence Research, Proceedings of the Summer Program* (Center for Turbulence Research, Stanford, CA, 1990), pp. 141–164.
[9] R. Sondergaard, J. H. Chen, J. Soria, and B. J. Cantwell, "Local topology of small scale motions in turbulent shear flows," in the Eighth Symposium on Turbulent Shear Flows, Munich, 9–11 September 1991.
[10] I. S. Gradshteyn and I. M. Ryzhik, *Table of Integrals Series and Products*, 4th ed. (Academic, New York, 1965).
[11] M. Abramowitz and I. Stegun, *Handbook of Mathematical Functions*, National Bureau of Standards Applied Mathematics Series 55 (Dover, New York, 1964).